

## Review Article

# Physicochemical and Electrical Properties of Praseodymium Oxides

**Sergio Ferro**

*Department of Biology and Evolution, University of Ferrara, Via L. Borsari 46, 44121 Ferrara, Italy*

Correspondence should be addressed to Sergio Ferro, fre@unife.it

Received 8 November 2010; Revised 28 February 2011; Accepted 21 March 2011

Academic Editor: Benjamin R. Scharifker

Copyright © 2011 Sergio Ferro. This is an open access article distributed under the Creative Commons Attribution License, which permits unrestricted use, distribution, and reproduction in any medium, provided the original work is properly cited.

The industrial research is continuously looking for novelties that could improve the applied processes, increasing the yields, lowering the costs, or improving the performances. In industrial electrochemistry, one more aspect is the stability of electrode materials, which is generally balanced by the catalytic activity: the higher the latter, the lower the former. A compromise has to be found, and an optimization is often the result of new ideas that completely change the way of thinking. Praseodymium-oxide-based cathodes have been proved to be quite interesting devices: the hydrogen evolution reaction is guaranteed by the presence of a noble metal (platinum and/or rhodium), while the stability and poisoning resistance seem to be strongly improved by the presence of lanthanide oxides.

## 1. Introduction

The reduction of costs, in terms of energy consumption and loading of precious metals for catalysts, is the main reason for the continuous research of more performing electrode materials. While the insoluble anodes adopted in the chlor-alkali industry have been investigated for some decades (starting from the pioneering works by Henry Beer in the seventies), the optimization of cathode performances is a recent request, and the research is still ongoing on this subject. At the moment, the membrane technology makes use of low-carbon steel cathodes, but both their relatively low exchange current density (high overpotential, i.e., from 300 to 400 mV) toward the hydrogen evolution reaction (HER) and their susceptibility to corrosion under the increasingly hard operating conditions (request for more concentrated sodium hydroxide solution production) have prompted for new materials. A significant reduction (from 100 to 200 mV) of HER overpotential has been obtained substituting the steel cathodes with nickel-based devices, possibly provided with catalytic coatings. However, the durability of such electrodes is limited, as the coating tends to dissolve, while impurities (mainly iron) are deposited on the electrode surface, reducing the catalytic activity.

In the last years, the industrial research has started investigating the behavior of devices provided with coatings in which a noble-metal catalyst is mixed with one or more oxides of lanthanide elements. A mixed platinum-cerium oxide coating has been claimed by Permelec Electrode Ltd. [1]: it is assumed that the cerium component has a crucial role in maintaining the catalytic activity of the noble metal, impeding the electrochemical deposition of iron; at the same time, the cerium oxide shows a good stability in concentrated alkali solutions.

Further stability improvements have been obtained with a catalytic layer containing at least three components, that is platinum, cerium, and lanthanum, in the form of metal, metal oxide or hydroxide [2]. From the examples discussed in the patent application, the ternary mixture shows performances that are not obtainable if one of the components is lacking (either a deterioration due to iron deposition or a high overvoltage is found).

A somewhat similar coating has been recently claimed by Industrie De Nora S.p.A.: the nickel substrate is provided with a first protective layer comprising palladium (as such or in mixture with silver), and a second, external layer containing a mixture of platinum or ruthenium with chromium or praseodymium oxide [3]. The first layer would

TABLE 1: Stoichiometry of the known members of the homologous series  $\text{Pr}_n\text{O}_{2n-2}$ . Reproduced from *J. Solid State Electrochem.*, 2001, 5, 531. Copyright 2001, Springer-Verlag [4].

Value of $n$	Formula	Phase	$x$ in $\text{PrO}_x$	Average oxidation state of Pr
4	$\text{Pr}_2\text{O}_3$	$\theta$	1.500	3.000
7	$\text{Pr}_7\text{O}_{12}$	$\iota$	1.714	3.428
9	$\text{Pr}_9\text{O}_{16}$	$\zeta$	1.778	3.556
10	$\text{Pr}_5\text{O}_9$	$\epsilon$	1.800	3.600
11	$\text{Pr}_{11}\text{O}_{20}$	$\delta$	1.818	3.636
12	$\text{Pr}_6\text{O}_{11}$	$\beta$	1.833	3.667
infinity	$\text{PrO}_2$		2.000	4.000

act as a sponge, absorbing hydrogen during the normal operation conditions and releasing it during the inversion events (accidental malfunctioning of the electrolyzer), thus preventing the cathode potential to be shifted to values high enough to give rise to significant dissolution phenomena. On the other hand, the presence of Cr or Pr oxides in the catalytic layer would preserve the catalyst activity, destroying the possible iron-based impurities while contributing to the film stability.

On the basis of the above information, the present paper aims at reviewing the role of praseodymium, while representing a possible starting point for further researches.

## 2. The Praseodymium Oxides

The oxides of praseodymium represent a system of phases whose composition is variable, although being restricted to a well defined range, and whose structure may be extensively defective. In addition to  $\text{Pr}_2\text{O}_3$  and  $\text{PrO}_2$ , at least other five suboxide phases have to be taken into consideration, and they represent a series of homologues having the  $\text{Pr}_n\text{O}_{2n-2}$  general composition (see Table 1) [4, 5].

Among the different phases,  $\text{Pr}_6\text{O}_{11}$  is the stable one at room temperature in air; also, it worth mentioning that the  $\text{Pr}_6\text{O}_{11}$  and  $\text{PrO}_{1.833}$  terminologies are completely equivalent (the former has not any special meaning).

Phases can be quite easily interconverted by means of a simple heating (or cooling) and suitably adjusting the oxygen content in the atmosphere in contact with the solid, as it can be inferred from Figures 1 and 2.

In addition, some scientific papers deal with the existence of intermediate phases ( $\text{PrO}_x$ ), in which  $x$  would assume the following values: 1.585, 1.658, and 1.703 [7, 8]; since the latter papers are quite aged, it is reasonable that some mistakes could have been done in the evaluation of data, and the examined phases could have been mixtures in which one phase has not completely converted into another.

In any case, the different phases differ for the dimension of the lattice parameters (see Figure 3) and, in some cases, also for the crystalline lattice and the color of the powder [5]: the  $\beta$  and  $\epsilon$  phases have a face-centered cubic lattice (*fcc*), with lattice constants of 5.468 and 5.481 Å, respectively; the former phase is black-colored, while the latter is brown.

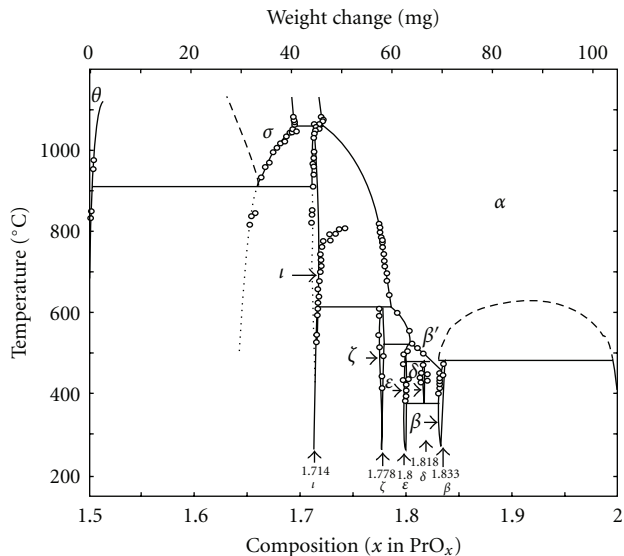


FIGURE 1: Projection of the phase diagram of the praseodymium-oxygen system on the temperature-composition plane. Reproduced from *Ionics*, 1999, 5, 426. Copyright 1999, Springer-Verlag [6].

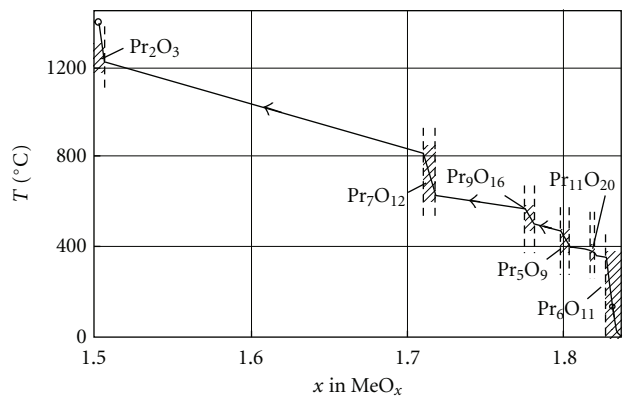
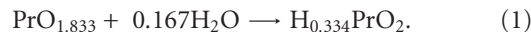


FIGURE 2: Relation between temperature and composition of the various phases in the praseodymium-oxygen system. Reproduced from *Ionics*, 1999, 5, 426. Copyright 1999, Springer-Verlag [6].

Also the  $\iota$  phase has a brownish color, but it presents a rhombohedral lattice with parameters  $a = 5.510 \text{ \AA}$  and  $\alpha$  slightly less than  $90^\circ$ . The  $\theta$  phase has a similar lattice (being *hexagonal*: side of the base hexagon =  $3.859 \text{ \AA}$ , height of the prism =  $6.008 \text{ \AA}$ ) but a different color, being yellow-green.

Finally, the  $\text{PrO}_2$  phase has a cubic lattice, with a fluorite structure; this phase is unstable and can be obtained by synthesizing the oxide under conditions of significant humidity or suspending the  $\text{Pr}_6\text{O}_{11}$  powder in boiling water for some hours [6]



Once the lattice vacancies have been saturated, an electrochemical reaction can still take place: oxygen is evolved as a gas, while protons and electrons enter the solid, causing the reduction of Pr(IV) ions to Pr(III). If water is removed,

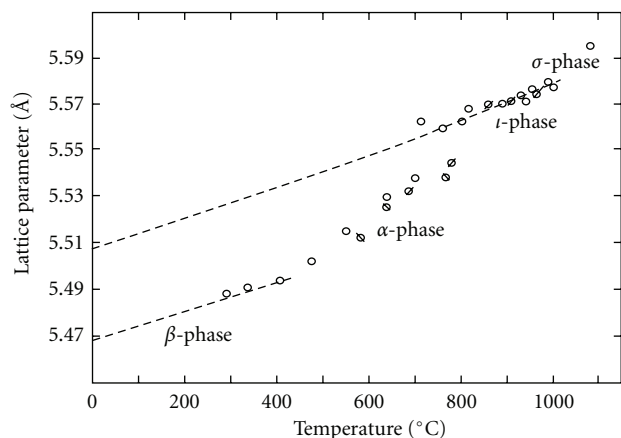


FIGURE 3: Lattice parameters of praseodymium oxide crystals as a function of temperature. Reproduced from *J. Phys. Chem.*, 1968, **72**, 4415. Copyright 1968, the American Chemical Society [5].

the material firstly changes into  $\text{PrO}_{1.5}$  but subsequently returns to the pristine  $\text{PrO}_{1.833}$  form, as a result of a spontaneous oxidation induced by the air.

For oxygen partial pressures close to the ambient conditions, the  $\beta$  phase is stable under  $430^\circ\text{C}$ : for higher temperatures, the oxide lattice expands [5] and the oxide progressively changes into  $\text{Pr}_{11}\text{O}_{20}$  (at about  $470^\circ\text{C}$ ),  $\text{Pr}_5\text{O}_9$  (at about  $490^\circ\text{C}$ ),  $\text{Pr}_9\text{O}_{18}$  (at about  $520^\circ\text{C}$ ), finally leading to the  $\text{Pr}_7\text{O}_{12}$  phase, as shown in Figure 4 (at  $700^\circ\text{C}$ ) [6].

### 3. Electrical and Thermal Properties

The electrical properties of the different phases differ by orders of magnitude: the  $\beta$  phase ( $\text{Pr}_6\text{O}_{11}$ ) shows a conductivity  $\sigma = 7.6 \times 10^{-6} \text{ S/cm}$  at  $60^\circ\text{C}$ , which significantly increases with the temperature (until  $850^\circ\text{C}$ ) to a value as large as  $1.40 \text{ S/cm}$ ; the  $\epsilon$  phase is far less conductive ( $\sigma$  is lower by three orders of magnitude), and the decrease is even more pronounced in the case of the  $\iota$  phase (in that case, the conductivity was not measurable, neither at  $600^\circ\text{C}$ ).

Generally speaking, the conductivity has been related to a mixed mechanism, which would involve both an ionic and an electronic transport (electron *hopping* between the mixed-valence ions present in the lattice) [4].

When the oxide is synthesized from a precursor salt, that is, for example, by the direct pyrolysis of  $\text{Pr}(\text{NO}_3)_3 \cdot 6\text{H}_2\text{O}$ , or through the preliminary formation of  $\text{Pr}(\text{OH})_3$  and a subsequent thermal treatment (e.g., at  $500^\circ\text{C}$  for one hour), the electrical conductivity seems to be inversely proportional to the dimension of crystallites: decreasing the dimension of grains, the effect of grain boundaries becomes significantly more important, affording the  $\text{Pr}_6\text{O}_{11}$  phase a greater conductivity [9]. It is worth mentioning that the above tests were carried out mixing the praseodymium oxide powders (88% in weight) with glassy carbon (6%) and polyvinylidene fluoride (6%), depositing the mixture onto an ITO-electrode (tin-doped indium oxide on glass) and evaporating the solvent firstly at  $120^\circ\text{C}$  per 30' and subsequently under vacuum at  $150^\circ\text{C}$  per 15 hours. The obtained results depend

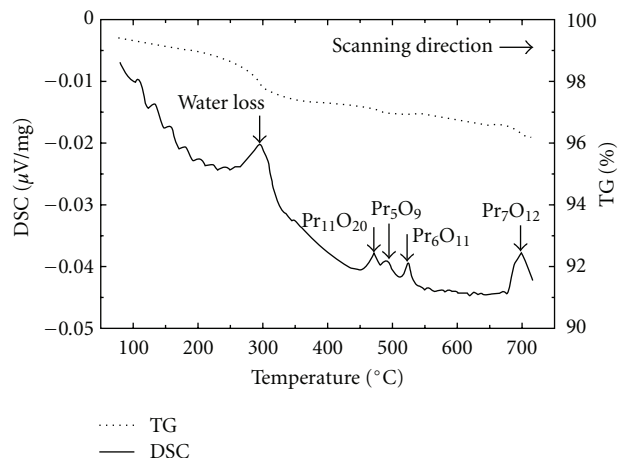


FIGURE 4: Results of thermal analysis of a sample of  $\text{Pr}_6\text{O}_{11}$ . Reproduced from *Ionics*, 1999, **5**, 426. Copyright 1999, Springer-Verlag [6].

on the suitability of the procedure, and data must be carefully interpreted.

Based on the experimental approach described in [10], both  $\text{Pr}_2\text{O}_{3+\delta}$  and  $\text{PrO}_{2-\delta}$  (where  $\delta$  is a small value) result to be insulators; the photoemission analysis investigation required the use of a *flood gun* for suppressing the electrostatic charging of specimens. On the basis of the above analysis, the concomitant presence of  $\text{Pr}^{3+}$  and  $\text{Pr}^{4+}$  ions, in the case of  $\text{PrO}_{2-\delta}$ , was established.

Interesting, because pertaining to the thermal decomposition of praseodymium nitrate (hydrate), is the paper by Hussein and coworkers [11]: the salt firstly melts and then progressively loses water, until the monohydrate compound is formed (the latter is thermally stable).

As shown in Figure 5, and schematized in Table 2, the subsequent loss of water requires a significant heating (from  $250^\circ\text{C}$  to  $340^\circ\text{C}$ ), and the anhydrous nitrate that is formed is then subjected to decomposition with evolution of  $\text{N}_2\text{O}_5$  (which, in its turn, decomposes into  $\text{NO}$ ,  $\text{NO}_2$ , and  $\text{O}_2$ ). At  $430^\circ\text{C}$ , the salt exists as an oxynitrate, which evolves to give  $\text{PrO}_{1.833}$ , as the final product, at  $465^\circ\text{C}$ .

The examination of the other papers available in the literature adds little information to what has been discussed so far; an XRD investigation [12], aimed at examining the region  $\text{PrO}_{1.833}\text{--PrO}_2$ , was carried out on specimens obtained from  $\text{Pr}_6\text{O}_{11}$ , autoclaved at temperatures between  $350^\circ\text{C}$  and  $760^\circ\text{C}$ , and in the presence of different amount of oxygen (from 0.2 to 230 atmospheres). On the basis of discussed results, the nominal composition of samples effectively varied in the examined range, but the XRD analysis showed that mixtures of the two limiting phases were present.

In consideration of the dielectrical characteristics of  $\text{Pr}_2\text{O}_3$ , further investigations were performed, aiming at the obtainment of thin films with high resistivity, to be used as sensors as well as in electronics.  $\text{Pr}_2\text{O}_3$  films can be grown using a metal-organic chemical vapor deposition (MO-CVD) technique; the temperature at which the substrate

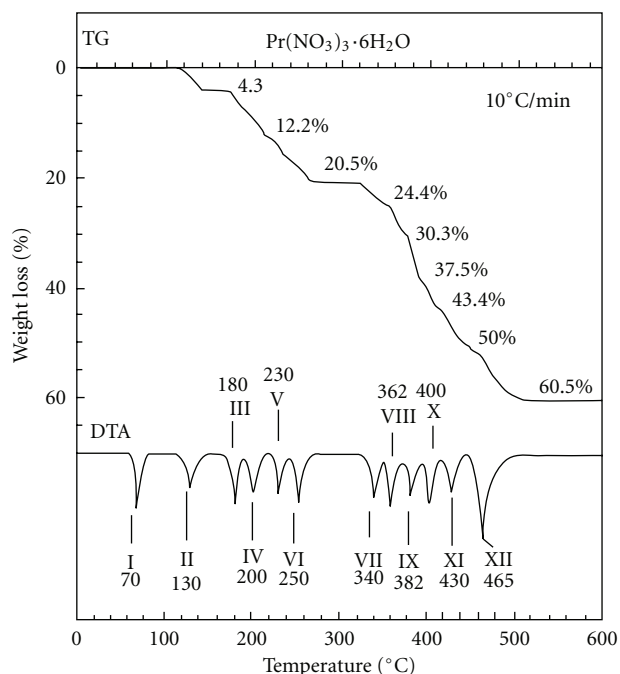


FIGURE 5: TG and DTA curves recorded for praseodymium nitrate at the heating rates indicated, in static air. Reproduced from *Thermoch. Acta*, 2001, **369**, 59. Copyright 2001, Elsevier [11].

is heated (between 450 and 850°C) decides for the film microstructure and its electrical properties. Only the specimens obtained at temperatures higher than 650°C appear completely crystalline; on the basis of data reported in [13], the estimated resistivity amounts to about  $7 \times 10^{10} \Omega \text{ cm}$ . Films obtained at lower temperatures are amorphous, and their resistivity is significantly lower ( $\rho \approx 4 \times 10^5 \Omega \text{ cm}$ ).

The above results are in agreement with data reported in [14], which pertain to crystalline films of  $\text{PrO}_x$  synthesized by *spray pyrolysis*, using the hydrate nitrate (previously discussed) as the precursor salt.

Thin films of  $\text{Pr}_6\text{O}_{11}$  can be obtained also through a cathodic deposition, by means of cyclic voltammetry, in media containing praseodymium nitrate and  $\text{H}_2\text{O}_2$  [15]; the synthesis was carried out onto ITO, cycling the electrode between 0.014 and  $-1.50 \text{ V}$  (versus  $\text{Ag}/\text{AgCl}$ ; scan rate:  $20 \text{ mV/s}$ ). Subsequently, the film was washed with water, dried in air, and treated in an oven at  $500^\circ\text{C}$  per one hour.

The interest on this material is also due to its possible use as a support [16], suitably “modifiable” with gold at the surface, for heterogeneous catalysis reactions (e.g., CO oxidation). While the paper has a quite “academic” character, the synthesis aimed at the preparation of  $\text{Pr}_6\text{O}_{11}$  nanotubes, starting from Pr metal, which was firstly dissolved in HCl and then treated with KOH, in order to precipitate the Pr hydroxide ( $K_{ps} = 3.39 \times 10^{-24}$  at  $25^\circ\text{C}$ ); the latter was autoclaved at  $180^\circ\text{C}$  per 45', dried, and then calcinated at  $600^\circ\text{C}$  per two hours. The gold-modified oxide is interesting in the oxidation reaction of CO, on accounting of the synergic action of gold nanoparticles and the presence of  $\text{Pr}_6\text{O}_{11}$  as an oxygen source.

TABLE 2: Pathway for the thermal decomposition of praseodymium nitrate in air. Reproduced from *Thermoch. Acta*, 2001, **369**, 59. Copyright 2001, Elsevier [11].

$\text{Pr}(\text{NO}_3)_3 \cdot 6\text{H}_2\text{O}$	$\xrightarrow{130^\circ\text{C}}$	$\text{Pr}(\text{NO}_3)_3 \cdot 5\text{H}_2\text{O}$
$\text{Pr}(\text{NO}_3)_3 \cdot 6\text{H}_2\text{O}$	$\xrightarrow{180^\circ\text{C}}$	$\text{Pr}(\text{NO}_3)_3 \cdot 4\text{H}_2\text{O}$
$\text{Pr}(\text{NO}_3)_3 \cdot 6\text{H}_2\text{O}$	$\xrightarrow{200^\circ\text{C}}$	$\text{Pr}(\text{NO}_3)_3 \cdot 3\text{H}_2\text{O}$
$\text{Pr}(\text{NO}_3)_3 \cdot 6\text{H}_2\text{O}$	$\xrightarrow{230^\circ\text{C}}$	$\text{Pr}(\text{NO}_3)_3 \cdot 2\text{H}_2\text{O}$
$\text{Pr}(\text{NO}_3)_3 \cdot 6\text{H}_2\text{O}$	$\xrightarrow{250^\circ\text{C}}$	$\text{Pr}(\text{NO}_3)_3 \cdot \text{H}_2\text{O}$
$\text{Pr}(\text{NO}_3)_3 \cdot 6\text{H}_2\text{O}$	$\xrightarrow{340^\circ\text{C}}$	$\text{Pr}(\text{NO}_3)_3$
$\text{Pr}(\text{NO}_3)_3 \cdot 6\text{H}_2\text{O}$	$\xrightarrow{362^\circ\text{C}}$	$\text{PrO}_{0.25}(\text{NO}_3)_{2.5}$
$\text{Pr}(\text{NO}_3)_3 \cdot 6\text{H}_2\text{O}$	$\xrightarrow{382^\circ\text{C}}$	$\text{PrO}_{0.5}(\text{NO}_3)_2$
$\text{Pr}(\text{NO}_3)_3 \cdot 6\text{H}_2\text{O}$	$\xrightarrow{400^\circ\text{C}}$	$\text{PrO}_{0.75}(\text{NO}_3)_{1.5}$
$\text{Pr}(\text{NO}_3)_3 \cdot 6\text{H}_2\text{O}$	$\xrightarrow{430^\circ\text{C}}$	$\text{PrO}(\text{NO}_3)$
$\text{Pr}(\text{NO}_3)_3 \cdot 6\text{H}_2\text{O}$	$\xrightarrow{465^\circ\text{C}}$	$\text{PrO}_{1.833}$

Similar principles are the base of the paper by Mullins [17]: a thin film (5 nm) of  $\text{Pr}_6\text{O}_{11}$  was synthesized onto a single crystal of ruthenium (preheated at  $700^\circ\text{K}$ ), by means of a thermal evaporation of Pr metal, in UHV, and in the presence of  $2 \times 10^{-7}$  torr of oxygen. Afterwards, the film was annealed at  $900^\circ\text{K}$ , and the obtained oxide, once decorated with metallic rhodium, was used to investigate the adsorption and the reactivity of both CO and ethylene.

Among the investigated precursors, for the synthesis of  $\text{PrO}_x$ , the thermal decomposition of the nitrate salt [9, 11, 14] and the calcination of the hydroxide [9, 15, 16] have been already discussed in the present paper; remaining in the same ambit, studies have been focused also on the thermal decomposition of the carbonate, either as such,  $\text{Pr}_2(\text{CO}_3)_3 \cdot 8\text{H}_2\text{O}$ , or after a reaction with citric acid (CA), which forms a complex with the metal ion [18]. Contrary to what happens in the case of the nitrate [11], the carbonate completely loses the water of crystallization in the temperature range between  $25^\circ\text{C}$  and  $152^\circ\text{C}$ . Subsequently, at about  $435^\circ\text{C}$ ,  $\text{Pr}_2\text{O}_2\text{CO}_3$  is formed, and this species remains stable for about 70 degrees, prior to the evolution of  $\text{CO}_2$  and the consequent formation of  $\text{PrO}_{1.833}$ , behind  $520^\circ\text{C}$ . As far as the Pr-CA complex is concerned, its stability seems to depend on the composition of the surrounding atmosphere: in the presence of a current of oxygen, the formation of  $\text{PrO}_{1.833}$  is quantitative already at  $450^\circ\text{C}$ ; at this temperature, but in the presence of nitrogen or in air (static conditions),  $\text{Pr}_2\text{O}_2\text{CO}_3$  is the major product (while heating in air, minor amounts of  $\text{PrO}_{1.833}$  are also produced).

The same species ( $\text{Pr}_2\text{O}_2\text{CO}_3$ ) is formed when the calcination procedure is performed starting from the hydrate acetate,  $\text{Pr}(\text{CH}_3\text{COO})_3 \cdot \text{H}_2\text{O}$ , or from the hydrate oxalate,  $\text{Pr}_2(\text{C}_2\text{O}_4)_3 \cdot 10\text{H}_2\text{O}$ , as reported in [19] and [20], respectively. Looking at the latter paper,  $\text{Pr}_2\text{O}_3$  is claimed to be useful as a selective dehydration catalyst, being capable of converting, for example, the 2-propyl alcohol into propene, at  $275^\circ\text{C}$ , with a 80% yield. On the contrary,  $\text{PrO}_{1.833}$  shows both dehydrating and dehydrogenating properties.

## 4. Electrochemical Applications

In electrode devices, the interest for praseodymium is substantially limited to two rather different fields: solid-oxide fuel cells (SOFCs) and hydrogen evolution reaction (HER) from strong alkaline solutions. In the first case, the element is a possible constituent of either a perovskite ( $ABX_3$ , where A and B are two cations of very different sizes, while X is an anion, generally oxygen, that bonds to both) or a spinel ( $AB_2O_4$ ) structure, and the complex oxide is of interest for its mixed (electronic/ionic) conductivity.

As previously discussed, the different praseodymium oxides may interconvert depending on temperature and oxygen partial pressure. Both these variables have a major role in SOFCs, and, in fact, a known limitation of Pr-based cathode materials is represented by the possible phase transitions and/or decompositions, which change the resistivity [21] as well as the physical properties of the material.

To stabilize the desired oxide structure, a suitable dopant may be added to the ceramic during its synthesis, as in the case of the perovskite-like compound  $Pr_{2-x}Sr_xNiO_{4\pm\delta}$  [22], where  $x$  is comprised between 0.3 and 0.6. The material is obtained by mixing  $Pr_6O_{11}$ ,  $SrCO_3$ , and  $NiO$  and ball-milling the mixture in a planetary mill for 4 h before the calcination step (at  $900^\circ\text{C}$ , for 6 h). The investigation was based on conductivity measurements at different  $O_2$  partial pressure and at different temperature. As anticipated, the insertion of strontium reduced the number of allowed transition phases, while increasing the electric conductivity and the stability of the perovskite toward the release of oxygen. As an example,  $Pr_{1.4}Sr_{0.6}NiO_{4\pm\delta}$  showed a quite high conductivity, around 100 S/cm, with a metal phase behavior—that is it decreased while increasing the temperature. Ceramic materials containing lanthanum ( $La_{2-x}Sr_xNiO_{4\pm\delta}$ ) showed conductivities that were lower by a 10%–15%, which is possibly justified by a less compact crystal structure, with respect to the Pr-containing compounds.

Rare-earth nickelates were also the subject of a more recent investigation, aiming at the optimization of the microstructure for increasing the performances and the stability of an SOFC cathode [23]. Among the investigated  $Ln_2NiO_{4\pm\delta}$  ( $Ln = La, Nd, \text{ and } Pr$ ) oxides, the Pr-based compound showed the highest diffusion coefficient for oxygen, as well as the largest amount of interstitial oxygen ( $\delta \approx 0.22$  at room temperature).

One more paper relating to SOFC is that by Yaroslavtsev and coworkers, who investigated lanthanum-strontium manganites modified with  $PrO_{2-x}$  [24]. In the authors' opinion, the presence of praseodymium oxide essentially accelerates the oxygen reaction; however, the electroactive  $PrO_{2-x}$  particles tend to sinter, causing a progressive decrease in the availability of reaction active sites.

The ionic conduction and the oxygen permeability are the reasons also for the utilization of  $Pr_2NiO_4$ -based oxides as membranes for the  $CH_4$  partial oxidation [25]. In that case, the oxygen permeation property of the perovskite-type oxide has been improved by inserting Fe and Cu as dopants in substitution of nickel. In particular, the partial replacement

of  $Ni^{2+}$  with  $Fe^{3+}$  allowed for an excess of oxygen in the oxide lattice, with respect to the stoichiometric amount.

As for the other subject matter (HER from alkaline media), most of available information relates to nickel alloys used as cathodes in water electrolysis. Tamura et al. reported that  $LaM_5$  ( $M = Ni, Co, \text{ and } Fe$ ) alloys have hydrogen overvoltages less negative than the corresponding M metals; in particular,  $LaNi_5$  showed an electrochemical activity (estimated through the logarithm of the exchange current density, extrapolating Tafel lines) almost comparable to that of platinum [26]. The different nickel alloys tend to absorb hydrogen, and the electrode surface may be severely damaged owing to hydrogen embrittlement. However, a proper choice of temperature and current density may partially eliminate the problem. In fact, the internal hydrogen fugacity, which corresponds to the hydrogen pressure in cavities in the electrode material, depends on cathodic overpotential, and thus on current density, and can be minimized by increasing the temperature.

The good performances of nickel-RE ( $RE = Y, Ce, Pr, \text{ and } Sm$ ) crystalline alloys were confirmed by Rosalbino et al., who investigated the HER in 1 M NaOH aqueous solution at room temperature [27]. As discussed also in [26], the Ni-RE systems show the ability to form hydrides with different stoichiometries, and, in fact, the Tafel slopes for the HER are generally around  $-0.18$  V/decade at prepolarized electrodes, and close to  $-0.12$  V/decade when measures are performed without prepolarization. In [27], the high electrocatalytic activity of Ni-RE has been tentatively ascribed to a spill over process involving coexisting Ni and  $Ni_5RE$  phases at the different electrode surface. Among the studied alloys,  $Ni_{94}Pr_6$  and  $Ni_{95}Ce_5$  showed the best behavior, as a possible result of a synergy between Ni and the  $Ni_5RE$  intermetallic compound.

Praseodymium, in the form of  $Pr_2O_3$ , has been further investigated by Yuan and coworkers as an additive for cathode devices based on nickel sulfur [28, 29]. The insertion of  $Pr_2O_3$  (or  $Er_2O_3$ ) in the Ni-S alloy increases the electrocatalytic activity for the HER in 30% KOH solutions at room temperature, but the effect is convincingly related to both a larger surface area and a more amorphous microstructure of the Ni-S coating added with  $Pr_2O_3$ .

Oxides with praseodymium at higher oxidation states, that is,  $Pr_7O_{12}$ ,  $Pr_6O_{11}$ , and  $PrO_2$ , were tested in nonaqueous organic solvent as possible cathodes for lithium batteries [30].  $Pr_6O_{11}$  was prepared by firing the oxalate precursor in air at  $800^\circ\text{C}$  for 6 h; a further thermal treatment in  $O_2$  at  $300^\circ\text{C}$  for 1 h led to the synthesis of  $PrO_2$ , while  $Pr_7O_{12}$  was prepared by heating  $Pr_6O_{11}$  in vacuum at  $580^\circ\text{C}$  for 1 h. Each  $PrO_x$  powder (296 mg) was mixed with graphite (80 mg), acetylene black (4 mg), and polyethylene powder (20 mg) and press-molded to obtain a tablet. Then, the electrolytic cell was filled with a 1:1 mixture of propylene carbonate and 1,2-dimethoxyethane, containing 1 mol/L of  $LiClO_4$ . The discharge curves of  $PrO_x$  cathodes showed remarkably better performance (the electrode potentials remain higher and longer) when increasing the oxygen content of the investigated cathode. However, during the discharge, the higher oxide was reduced to the lower, liberating unstable lattice oxygen atoms, which were consumed to form  $Li_2O$ .

A final paper deserving a comment, at least for its electrochemical character, is that by Mari et al. [31], which deals again with  $\text{Pr}_2\text{NiO}_4$  films. The oxide is formed starting from  $\text{PrCl}_3$ , which is initially converted into the pertaining nitrate and then added to a solution of  $\text{Ni}(\text{NO}_3)_2$ ; once the solvent has been evaporated, the salt is decomposed at  $300^\circ\text{C}$ – $500^\circ\text{C}$  and subsequently calcinated at even higher temperatures ( $1100^\circ\text{C}$ – $1300^\circ\text{C}$ ). Supported thin films were analogously prepared onto platinum foils, starting from the nitrate solution.

The most interesting part of the investigation relates to the electrochemical behavior of supported films in aqueous solutions: the study was carried out by means of cyclic voltammeteries (in 1 M NaOH, at  $25^\circ\text{C}$ ) and polarization curves. In the former case, the explored potentials were chosen between  $-200$  and  $+500$  mV (versus SCE), and the obtained curves showed a couple of signals, plausibly related to variations of the VIII B-metal oxidation state (e.g., a redox transition from NiO to  $\text{Ni}_2\text{O}_3$ ). On the other hand, the kinetic analysis was limited only to positive potential values for the investigation of the oxygen evolution reaction: while the electrode material showed significant analogies with platinum, the cyclic variation of potentials led to irreversible degradation.

The latter remark is in agreement with the pieces of information reported by Pourbaix, concerning the features of both Pr and Ni: while the former is chemically stable, as an oxide/hydroxide (and for pH more alkaline than 9–9.5), in the potential region from about  $-3$  to about  $+0.6$  V, the latter tends to corrode, for pH  $> 12$ , at potentials from  $-1$  to about  $0.3$  V [32].

## 5. Conclusions

In conclusion, there is certainly space for further research on the physicochemical and electrical properties of praseodymium oxides, mostly because the available information on the behavior of  $\text{PrO}_x$  as cathode material for the HER from alkaline solutions is rather poor. In [3], it has been suggested that the high oxidizing power of praseodymium oxide is beneficial for stabilizing the catalytic metal (Pt, Ru, and/or Rh), while in [1], it is assumed that sparingly soluble cerium hydroxide is formed in highly concentrated alkali; when the device is used as a cathode in a chlor-alkali cell, the Ce-based coating also hinders the electrochemical deposition of metal poisons (e.g., iron) onto the catalytic component. In both cases, the role of the rare-earth oxide has not been properly elucidated. As discussed in this paper, praseodymium can form different compounds (oxides, perovskites, and metallic alloys), but the preparation conditions reported in [3] considerably limit the achievable outcome. While the acidity of the precursor solutions would allow the superficial dissolution of the substrate (nickel) and the formation of a mixed phase (which is also desirable for obtaining a good adhesion between the coating and the substrate), the formation of  $\text{Pr}_2\text{NiO}_4$  is almost certainly minimized by the presence of the intermediate layer. In [3], the stability of the catalytic layer containing praseodymium oxide was demonstrated and compared to other coating

compositions, comprising that of [1]; at a first attempt of characterization, the nature of  $\text{PrO}_x$  in that device is still unknown, the XRD pattern being completely different from that of  $\text{Pr}_6\text{O}_{11}$  [33].

This seems to replicate what happened with the Beer's dimensionally stable anodes: the proposed devices were industrially tested and applied well before the academy could start to investigate them, trying to elucidate their properties.

## References

- [1] Y. Nishiki, S. Nakamatsu, and T. Shimamune, US patent, 5 035 779, 1991.
- [2] M. Nara, T. Suzuki, M. Tanaka, and Y. Nishiki, US patent application US 2009/0223815, 2009.
- [3] A. L. Antozzi, C. J. Bargioni, A. Calderara, L. Iacopetti, G. N. Martelli, and C. Urgeghe, US patent application US 2009/0194411, 2009.
- [4] V. Thangadurai, R. A. Huggins, and W. Weppner, "Mixed ionic-electronic conductivity in phases in the praseodymium oxide system," *Journal of Solid State Electrochemistry*, vol. 5, no. 7-8, pp. 531–537, 2001.
- [5] D. A. Burnham and L. Eyring, "Phase transformations in the praseodymium oxide-oxygen system: high-temperature X-ray diffraction studies," *Journal of Physical Chemistry*, vol. 72, no. 13, pp. 4415–4424, 1968.
- [6] A. Netz, W. F. Chu, V. Thangadurai, R. A. Huggins, and W. Weppner, "Investigations of praseodymium oxide electrodes in lithium concentration cells," *Ionics*, vol. 5, no. 5-6, pp. 426–433, 1999.
- [7] R. L. Martin, "Oxides of praseodymium," *Nature*, vol. 165, no. 4188, pp. 202–203, 1950.
- [8] C. T. Stubblefield, H. Eick, and L. Eyring, "Praseodymium oxides. III. The heats of formation of several oxides," *Journal of the American Chemical Society*, vol. 78, no. 13, pp. 3018–3020, 1956.
- [9] S. Shrestha, C. M. Y. Yeung, C. Nunnerley, and S. C. Tsang, "Comparison of morphology and electrical conductivity of various thin films containing nano-crystalline praseodymium oxide particles," *Sensors and Actuators, A*, vol. 136, no. 1, pp. 191–198, 2007.
- [10] S. I. Kimura, F. Arai, and M. Ikezawa, "Mixed valence of praseodymium oxides," *Journal of Electron Spectroscopy and Related Phenomena*, vol. 78, pp. 135–138, 1996.
- [11] G. A. M. Hussein, B. A. A. Balboul, M. A. A-Warith, and A. G. M. Othman, "Thermal genesis course and characterization of praseodymium oxide from praseodymium nitrate hydrate," *Thermochimica Acta*, vol. 369, no. 1-2, pp. 59–66, 2001.
- [12] C. L. Sieglaff and L. Eyring, "Praseodymium Oxides. IV. A study of the region  $\text{PrO}_{1.83}$ – $\text{PrO}_{2.00}$ ," *Journal of the American Chemical Society*, vol. 79, no. 12, pp. 3024–3026, 1957.
- [13] R. L. Nigro, R. G. Toro, G. Malandrino, P. Fiorenza, V. Raineri, and I. L. Fragalà, "Effects of deposition temperature on the microstructural and electrical properties of praseodymium oxide-based films," *Materials Science and Engineering B*, vol. 118, no. 1-3, pp. 117–121, 2005.
- [14] P. A. Tikhonov, A. T. Nakusov, I. A. Drozdova, M. V. Kalinina, and A. I. Domanskii, "Investigation into the sensory properties of fine-grain polycrystalline films based on cobalt, nickel, and praseodymium oxides," *Glass Physics and Chemistry*, vol. 31, no. 5, pp. 700–708, 2005.

- [15] S. Shrestha, F. Marken, J. Elliott, C. M. Y. Yeung, C. E. Mills, and S. C. Tsang, "Electrochemical deposition of praseodymium oxide on tin-doped indium oxide as a thin sensing film," *Journal of the Electrochemical Society*, vol. 153, no. 7, pp. C517–C520, 2006.
- [16] P. X. Huang, F. Wu, B. L. Zhu et al., "Praseodymium hydroxide and oxide nanorods and Au/Pr<sub>6</sub>O<sub>11</sub> nanorod catalysts for CO oxidation," *Journal of Physical Chemistry B*, vol. 110, no. 4, pp. 1614–1620, 2006.
- [17] D. R. Mullins, "Adsorption of CO and C<sub>2</sub>H<sub>2</sub> on Rh-loaded thin-film praseodymium oxide," *Surface Science*, vol. 556, no. 2-3, pp. 159–170, 2004.
- [18] M. Popa and M. Kakihana, "Praseodymium oxide formation by thermal decomposition of a praseodymium complex," *Solid State Ionics*, vol. 141-142, pp. 265–272, 2001.
- [19] G. A. M. Hussein, "Formation of praseodymium oxide from the thermal decomposition of hydrated praseodymium acetate and oxalate," *Journal of Analytical and Applied Pyrolysis*, vol. 29, no. 1, pp. 89–102, 1994.
- [20] G. A. M. Hussein, "Characterisation and activity of praseodymium oxide catalysts prepared in different gases from praseodymium oxalate hydrate. Microscopic, thermogravimetric and IR spectroscopic studies," *Journal of the Chemical Society, Faraday Transactions*, vol. 91, no. 9, pp. 1385–1390, 1995.
- [21] P. Odier, C. H. Allançon, and J. M. Bassat, "Oxygen exchange in Pr<sub>2</sub>NiO<sub>4+δ</sub> at high temperature and direct formation of Pr<sub>4</sub>Ni<sub>3</sub>O<sub>10-x</sub>," *Journal of Solid State Chemistry*, vol. 153, no. 2, pp. 381–385, 2000.
- [22] V. Vashook, J. Zosel, T. L. Wen, and U. Guth, "Transport properties of the Pr<sub>2-x</sub>Sr<sub>x</sub>NiO<sub>4+δ</sub> ceramics with x = 0.3 and 0.6," *Solid State Ionics*, vol. 177, no. 19-25, pp. 1827–1830, 2006.
- [23] C. Ferchaud, J.-C. Grenier, Y. Zhang-Steenwinkel, M. M.A. Van Tuel, F. P.F. Van Berkel, and J.-M. Bassat, "High performance praseodymium nickelate oxide cathode for low temperature solid oxide fuel cell," *Journal of Power Sources*, vol. 196, no. 4, pp. 1872–1879, 2011.
- [24] I. Y. Yaroslavtsev, B. L. Kuzin, D. I. Bronin, G. K. Vdovin, and N. M. Bogdanovich, "Cathodes based on (La, Sr)MnO<sub>3</sub> modified with PrO<sub>2-x</sub>," *Russian Journal of Electrochemistry*, vol. 45, no. 8, pp. 875–880, 2009.
- [25] T. Ishihara, S. Miyoshi, T. Furuno, O. Sanguanruang, and H. Matsumoto, "Mixed conductivity and oxygen permeability of doped Pr<sub>2</sub>NiO<sub>4</sub>-based oxide," *Solid State Ionics*, vol. 177, no. 35-36, pp. 3087–3091, 2006.
- [26] H. Tamura, C. Iwakura, and T. Kitamura, "Hydrogen evolution at LaNi<sub>5</sub>-type alloy electrodes," *Journal of The Less-Common Metals*, vol. 89, no. 2, pp. 567–574, 1983.
- [27] F. Rosalbino, G. Borzone, E. Angelini, and R. Raggio, "Hydrogen evolution reaction on Ni-RE (RE = rare earth) crystalline alloys," *Electrochimica Acta*, vol. 48, no. 25-26, pp. 3939–3944, 2003.
- [28] T. Yuan, K. Zhou, and R. Li, "Effect of Pr<sub>2</sub>O<sub>3</sub> on the microstructure and hydrogen evolution property of nickel sulphur coatings electrodeposited on the nickel foam substrate," *Materials Letters*, vol. 62, no. 19, pp. 3462–3464, 2008.
- [29] T.-C. Yuan, K.-C. Zhou, and R.-D. Li, "Effect of additives Pr<sub>2</sub>O<sub>3</sub> and Er<sub>2</sub>O<sub>3</sub> on properties of electrodeposited nickel sulphur alloy electrode," *Zhongguo Yuese Jinshu Xuebao*, vol. 18, no. 5, pp. 862–866, 2008.
- [30] Y. Takasu, Y. Matsuda, and K. Yamashita, "The contribution of lattice oxygen atoms of praseodymium oxide to its cathodic performance," *Chemistry Letters*, vol. 10, pp. 1339–1340, 1981.
- [31] C. Mari, V. Scolari, G. Fiori, and S. Pizzini, "Structural, electrical and electrochemical characterization of Ni-Pr oxide thick films," *Journal of Applied Electrochemistry*, vol. 7, no. 2, pp. 95–106, 1977.
- [32] M. Pourbaix, *Atlas d'Équilibres Électrochimiques*, 1963.
- [33] S. Ferro, unpublished results.



**Hindawi**

Submit your manuscripts at  
<http://www.hindawi.com>

